

# Analysis of Satellite Constellations for the Continuous Coverage of Ground Regions

Guangming Dai,<sup>a</sup> Xiaoyu Chen,<sup>b</sup> and Maocai Wang,<sup>c</sup>  
*China University of Geosciences, Wuhan CO 430074, China*

Elena Fernández,<sup>d</sup>  
*Technical University of Catalonia, Barcelona, CO 08034, Spain*

Tuan Nam Nguyen,<sup>e</sup> and Gerhard Reinelt,<sup>f</sup>  
*Heidelberg University, Heidelberg, CO 69120, Germany*

This paper studies the problem of analyzing multisatellite constellations with respect to their coverage capacity of areas on Earth's surface. The geometric configuration of constellation projection points on Earth's surface is investigated. A geometric subdivision approach is described, and the coverage target area belonging to each satellite and its maximum circle radius are defined and calculated. Accordingly, the target area can be decomposed into subregions, and thus the multisatellite coverage problem is decomposed into a one-satellite coverage problem. An accurate and effective solution method is proposed that solves both continuous and discontinuous coverage problems for any type of ground area. In addition, a procedure for calculating satellite orbital parameters is also proposed. The performance of our approach is analyzed using the Globalstar system as an example, and it is shown that it compares favorably with the classical grid-point technique and the longitude method.

<sup>a</sup> Prof. Dr., School of Computer Science, [cugdgm@126.com](mailto:cugdgm@126.com).

<sup>b</sup> Ph.D., School of Computer Science, [xiaoyu.chen@informatik.uni-heidelberg.de](mailto:xiaoyu.chen@informatik.uni-heidelberg.de). (Corresponding author)

<sup>c</sup> Ass.Prof. Dr., School of Computer Science, [cugwangmc@126.com](mailto:cugwangmc@126.com).

<sup>d</sup> Prof. Dr., Statistics and Operations Research Department, [e.fernandez@upc.edu](mailto:e.fernandez@upc.edu).

<sup>e</sup> Dr., Institute of Computer Science, [namtn.fami@gmail.com](mailto:namtn.fami@gmail.com).

<sup>f</sup> Prof. Dr., Institute of Computer Science, [ip121@uni-heidelberg.de](mailto:ip121@uni-heidelberg.de).

## Nomenclature

$O_e$	$=$	Earth's center
$R_e$	$=$	Earth's radius
$S$	$=$	the satellite
$\mathcal{C}$	$=$	the satellites constellation
$H$	$=$	orbital altitude
$P, P'$	$=$	point on Earth's surface
$\gamma_{min}$	$=$	minimum elevation angle
$\alpha$	$=$	coverage angle
$d$	$=$	coverage spherical radius
$r$	$=$	spherical circumcircle radius
$\mathcal{O}$	$=$	the finite set in some metric space $\mathcal{M}$ with distance function $d$
$VR(O_i)$	$=$	the Voronoi region associated with the point $O_i$
$VD(\mathcal{O})$	$=$	the Voronoi diagram of $\mathcal{O}$
$DT(\mathcal{O})$	$=$	the Delaunay triangulation of $\mathcal{O}$
$\Theta(P, \alpha)$	$=$	spherical circle with the center point $P(\theta, \varphi)$ and radius $\alpha$
$\theta, \varphi$	$=$	the longitude and latitude angle
$\mathcal{M}(P)$	$=$	coordination rotation matrix in $\mathbb{R}^{3 \times 3}$
$R_u(\alpha)$	$=$	the rotation with angle $\alpha$ around the $u$ -axis
$\beta$	$=$	the orientation angle
$g(\beta)$	$=$	one-to-one mapping from $\beta$ to a unique point
$h(\Theta')$	$=$	projection function from a spherical $h(\Theta')$ to the $yz$ -plane
$f$	$=$	mapping an orientation angle to a point on the spherical circle
$\Omega$	$=$	target area
$\Omega_i$	$=$	the coverage target area of $S_i$
$\partial\Omega_i$	$=$	the boundary of coverage target area $\Omega_i$
$r_{max}(i)$	$=$	maximum circle radius of $S_i$
$F_i$	$=$	the coverage feature point set of $S_i$

## I. Introduction

SATELLITES find numerous applications in communication, navigation, imaging, and remote sensing [1, 2]. The requirements for data accuracy and real-time observations become more and more extensive as the need for Earth's observation data continuously increases [3]. To satisfy these demands systems of multiple satellites have to be designed and their performance has to be analyzed.

Earth observation from remote satellites and data transmission between satellites and facilities are both related to *satellite coverage*. In general, satellite coverage problems arise when a target area on the Earth's surface must be visible to one or more satellites. In principle, there are two main types of coverage problems. One class assumes that the parameters of the satellites is fixed and studies their *coverage capacity* measured in terms of the percentage of the target area which is covered (visible). The second class of problems refers to the determination of the positions of the satellites (i.e., their *constellation* or *configuration*) including satellites orbital parameters in order to achieve a maximum coverage. Special variants arise in both settings if *full coverage* of the target area is requested and an accurate determination of the achieved coverage is necessary with respect to a variety of coverage areas. Furthermore, because satellites are moving and covering areas are subject to change, in practice these problems must be extended to account for varying constellations within given time intervals, also denoted *reconstruction periods*.

Most methods in coverage analysis are based on the visibility of a subset of points of the given target area [4]. Hence, an accurate coverage of such points becomes a prerequisite, given that the performance of satellite constellations significantly depends on the precision with which such points are covered. Recent research on coverage analysis often resorts to simulation or analytical methods. Such methods exhibit a low computational efficiency and little reliability of the results. Thus alternative methods are needed for large target areas when high accuracy is required.

In this paper we present a method to obtain the coverage target area and coverage capacity for each satellite of a constellation. The method is based on a geometric subdivision of the target area obtained from the spherical Voronoi diagram and its associated Delaunay triangulation. Our geometric subdivision method also allows to compute directly the satellites orbital parameters when full coverage is imposed. From the coverage areas obtained for a fixed time point, the full coverage

and the continuous coverage capacity can be efficiently and accurately computed in the desired reconstruction period. Overall, the constellation design process improves significantly. Furthermore, our method is very versatile as it solves discontinuous and continuous coverage problems for any type of target areas.

This paper is organized as follows. Section II reviews some related literature and Section III introduces the main concepts related to satellite coverage of a ground region. In Section IV we review the properties of two classical geometric structures and define the orientation angle. Section V defines the coverage target area belonging to a single satellite, and presents a computational approach for the analysis of the continuous coverage area associated with multi-satellites. In section VI we give a method for the computation of orbital parameters when full coverage is imposed. The results assessing the correctness and the efficiency of the proposed methods using the Globalstar system as an example are presented in Section VII [5], where we also compare the performance of our approach with two popular coverage methods. The paper ends in Section VIII with a summary and some conclusions.

## II. Literature Review

In 1970, Walker [6] studied circular orbital patterns and particular constellation configurations for the continuous coverage of global regions, ensuring that every point on the Earth's surface is always visible from at least one satellite, under the constraint of the minimum elevation angle. Crossley and Williams [7] proposed simulated annealing and genetic algorithms for the same problem. Asvial et al. [8] addressed the design of constellation configurations taking into account the total number of satellites and their altitudes, the angle shift between satellites, the angle between planes, and the inclination angle. Multi-objective evolutionary algorithms, dealing with the discrete and nonlinear characteristics of the metrics, have been developed for the design of satellite constellations for regional coverage by Ferringer and Spencer [9] and by Wang et al. [10]. Ferringer et al. [11] proposed two parallel multi-objective evolutionary algorithmic frameworks (master-slave and island approach) for the same problem, which approximate the true Pareto frontier.

One challenge when applying evolutionary algorithms to constellation design is how to incorporate suitably satellite kinematical features and constellation coverage characteristics relevant to the

optimization process. Given that satellite orbitals are determined by six parameters which need to be repeatedly coded and updated, large computing times and memory space are usually required. Thus, when addressing constellation design, it seems more suitable to only consider a few satellites together with coverage requirements for a series of point-targets.

From a methodological point of view, recent research on Earth coverage analysis can be classified as numerical simulation or analytical methods. Currently, the grid-point technique is the most commonly used method for satellite coverage analysis in several applications [12–14]. This technique was first introduced in early 1973 by Morrison [15] for the percentage satellite coverage on the Earth’s surface, and for the statistical analysis of the full coverage of a region for a system with sixteen synchronous satellites. For the evaluation of the satellite coverage capacity Jiang et al. [16] computed the percentage coverage of a ground region by a constellation at any time by *(i)* dividing the target area into a number of discrete grids according to certain rules, and *(ii)* taking the satellite’s coverage capacity to the center of each grid as the coverage capacity for the entire grid area. Mortari et al. [17] applied the Flower constellation theory to the maximization of the global coverage and the network connectivity via inter-satellite links. On the other hand, Casten et al. [18] modeled the Earth’s surface as a series of longitudinal strips and investigated the cumulative coverage problem by determining the exact latitude intervals that must be observed at each time instant. The accuracy of the method only depends on the choice of the time step and the number of strips that are used for instantaneous coverage computations. More recently, Xu and Huang [19] proposed a new algorithm for the design of revisited orbitals in satellite coverage. In particular, they analyzed the global coverage performance and the relationship between the coverage percentage and the orbital altitude by mapping every orbit pass into its ascending and descending nodes on different latitude circles, and by evaluating the performance at different altitudes. For the constraint on the elevation angle, Ulybyshev et al. [20] and Seyedi et al. [21] proposed statistical methods for the computation of satellite coverage times and service areas, based on the analysis of satellites coverage capacity to each latitude. Such procedures eliminate the errors of traditional techniques, due to points with discrete values in the latitude direction.

The Rosette Constellation [22] was proposed by Ballard in the 1980s based on a concept different

from numerical simulation. This method presents better constellation coverage properties, which are analyzed in terms of the largest coverage circle range between anywhere on the Earth's surface and the nearest subpoint of the satellite. In [23, 24] authors introduce specific methods implemented for particular cases of discontinuous coverage analysis. they are still associated with the calculating procedure with a priori selected classes of orbital structures or the particular character of the Earth surface coverage type. Mozhaev [25] analyzed the kinematics of the specific inter-satellites constellation and studied a single continuous global coverage problem using symmetry group theory. Ulybyshev [4] defined a function for the (full or partial) coverage capacity of a satellite for a geographical region, which uses as parameters the right ascension of ascending node (RAAN) and the latitude. In [26, 27] the same author introduced a geometric pattern, named coverage belt, and developed a new method for the analysis of maximum revisiting times to a specified latitude in discontinuous coverage satellite constellations. Razoumny [28] analysed and investigated the satellite constellation design for Earth discontinuous coverage based on the geometry analytic solutions for latitude coverage by single satellite. Mohammadi [29] introduced the concept of the best coverage region for the receiving stations from a low Earth orbit (LEO) remote sensing satellite. He proposed a construction method guaranteeing the requirements of the receiving stations, based on the analysis of the variation of the satellite's altitude for the coverage areas obtained under different minimum elevation angle constraints. In this approach, the best coverage region is defined as the coverage area of the satellite. Sengupta et al. [30] proposed a semi-analytical technique for the study of the coverage of LEO satellites. They expressed the coverage area of a satellite as a function of orbital elements, and obtained accurate results using numerical integration methods. The above-mentioned simulation methods are usually time-consuming and of low accuracy. Analytical methods are only used for the continuous coverage analysis of a single satellite and regular target areas (e.g., a single point, a latitude or longitude line, or the global region). They are used for analyzing the coverage performance of a single satellite and are exact over time only if the orbital parameters are analyzable, but they are not suitable for calculating the coverage capacity of satellite constellations for any specified ground areas.

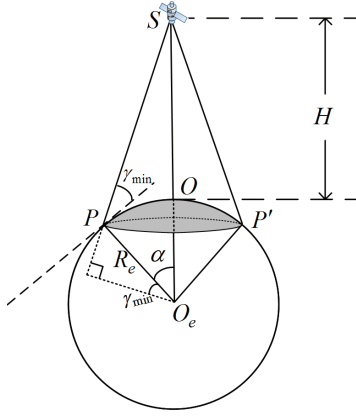


Fig. 1: Coverage area of a satellite

on Earth.

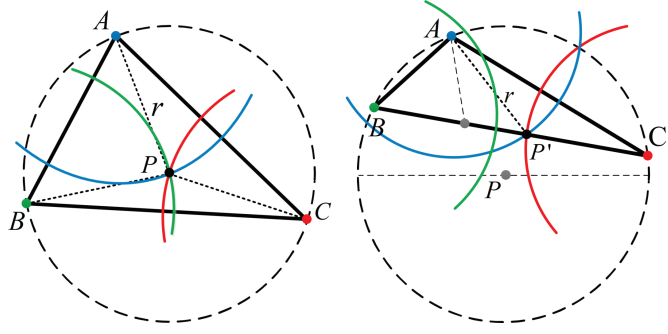


Fig. 2: Spherical triangle defined by three satellites.

### III. Basic Coverage Definitions and Properties

For our purposes Earth is assumed to be a perfect sphere with center  $O_e$  and radius  $R_e$ . For a satellite  $S$  and a point  $P$  on Earth's surface visible from  $S$ , the *elevation angle* at  $P$  is the angle between the line connecting  $S$  and  $P$  and the tangent plane to the Earth's surface at  $P$ . The *subpoint*  $O$  of  $S$  is the projection of  $S$  on the surface and is the unique point on the Earth's surface with elevation angle  $\pi/2$ . It is obtained by intersecting the line connecting  $S$  and  $O_e$  with the Earth's surface. The *coverage area* of  $S$  contains all the points on the Earth's surface that can be observed from  $S$  with elevation angle of at least  $\gamma_{\min}$  and is determined by a spherical circle (shaded part of Figure 1) associated with the *coverage angle*  $\alpha$  whose spherical radius is  $d = R_e \alpha$ . Figure 1 illustrates the *coverage area* for a typical observation activity of a satellite  $S$  located at an *orbital altitude*  $H$  for a *minimum elevation angle*  $\gamma_{\min}$ . The well-known relation of the coverage angle  $\alpha$  with the orbital altitude  $H$  and the minimum elevation angle  $\gamma_{\min}$  is given by

$$\alpha = \arccos\left[\frac{R_e \cos(\gamma_{\min})}{R_e + H}\right] - \gamma_{\min}. \quad (1)$$

Relation (1) indicates that, for the case of one single satellite, when the minimum elevation angle  $\gamma_{\min}$  is fixed, the size of the coverage circle only depends on the orbital altitude  $H$  of the satellite.

Consider now three satellites at the same orbital altitude. Let  $A$ ,  $B$ , and  $C$  denote their respective subpoints. Since all satellites are at the same orbital altitude, their coverage areas have the same spherical radius  $d$ . Let  $\triangle ABC$  be the spherical triangle on the Earth's surface defined

by these points and let  $P$  and  $r$  be, respectively, the center and radius of the spherical circumcircle of  $\triangle ABC$ . Furthermore let  $P'$  denote the point in  $\triangle ABC$  that minimizes the maximum of the distances to  $A, B$ , and  $C$ . Note that when  $P' \in \triangle ABC$ , then  $P'$  coincides with  $P$ . Otherwise  $P'$  is a point in the perimeter of  $\triangle ABC$ . The two cases are illustrated in Figure 2, where the coverage areas of satellites  $A, B$ , and  $C$  intersecting  $\triangle ABC$  are delimited by the blue, green and red arcs, respectively. The exact definition and generation approach will be given below.

Thus, in order to have full coverage of  $\triangle ABC$  with the three satellites it is enough to ensure that the point  $P'$  is covered, i.e., that  $d \geq r$ .

This condition can be extended to the case of a constellation consisting of multiple satellites in circular orbit at the same orbital altitude. Suppose that the Earth's surface can be divided into several adjacent spherical triangles (with pairwise disjoint interiors) by connecting the subpoints of the satellites according to certain rules (see Section IV). Then, only the points  $P'_i$  and the maximum distance  $r_i$  of each spherical triangle must be computed, and if the coverage radius  $d$  of the satellites satisfies

$$d \geq \max\{r_1, r_2, \dots, r_N\}, \quad (2)$$

then this proves that the constellation covers the surface of the Earth completely.

Note that the coverage radius  $d$  is a technical parameter of a satellite. This parameter is denoted as *coverage angle*  $\theta$  introduced in [20]. However, the *Earth-central angle*  $\vartheta$  that is defined in the first covering function of [20] considered for the arbitrary points of a given latitude, whereas the *maximum circle radius*  $r$  of a satellite that is defined and computed based on two geometric structures (see Section V) is the maximum spherical distance between its subpoint and any point in its coverage target area. This kind of analysis will be extended to any type of coverage areas on Earth's surface, provided that it can be divided into several adjacent spherical convex polygons (according to certain rules). Also in such cases it will be easy to determine whether or not the constellation can completely cover the ground area. Moreover, if condition (2) holds for a given constellation at any time of a given reconstruction period, then the constellation fulfills the single continuous coverage property for the given ground area.



## IV. Spherical Geometric Subdivision

### A. Voronoi Diagrams and Delaunay Triangulations

The Voronoi diagram and the Delaunay triangulation are two classical geometric structures in computational geometry [31, 32], which produce partitions of a given region or set of points in a metric space. Because of their interesting properties they are widely used in various areas such as multispectral sensor image processing. Moreover, the closest point property of Delaunay triangulations is iteratively used in several graph matching and image registration methods, like the ones proposed by Zhao et al. [33].

The general definition of a Voronoi diagram is as follows. Let  $\mathcal{O} = \{O_1, O_2, \dots, O_n\}$  be a finite set of points (set of *generators*) in some metric space  $\mathcal{M}$  with distance function  $d$ . The *Voronoi region* associated with the point  $O_i$  is the set  $VR(O_i) = \{O \in \mathcal{M} \mid d(O, O_i) \leq d(O, O_j), \text{ for } j = 1, \dots, N, j \neq i\}$ , i.e., the set of points for which  $O_i$  is closest among the generators. The set of all  $N$  Voronoi regions is called the *Voronoi diagram*  $VD(\mathcal{O})$  of  $\mathcal{O}$ . It gives a partition of  $\mathcal{M}$  into polygons with mutually disjoint interiors.

For a given Voronoi diagram of  $\mathcal{O}$  the corresponding *Delaunay triangulation*  $DT(\mathcal{O})$  of  $\mathcal{O}$  is obtained if two points in  $\mathcal{O}$  are connected by a shortest line if and only if their corresponding Voronoi regions have a nonempty intersection. Under appropriate conditions which are usually satisfied, two Voronoi regions do not intersect at all or intersect in more than one point and  $DT(\mathcal{O})$  has  $3N - 6$  edges defining  $2N - 4$  triangles covering the space  $\mathcal{M}$  (where triangles can only intersect in lines) [22]. The Delaunay triangulation thus also provides a partition of  $\mathcal{M}$  (into triangles with mutually disjoint interiors).

Both concepts are dual to each other. It is also possible to first compute the Voronoi diagrams directly and then obtain the Delaunay triangulation. There are many efficient algorithms for computing either of the two and we do not elaborate on them here [34–37].

In our application we have a constellation of  $N$  satellites  $\mathcal{C} = \{S_1, S_2, \dots, S_N\}$  and we consider Voronoi diagram and Delaunay triangulation for the set  $\mathcal{O} = \{O_1, O_2, \dots, O_N\}$  of their respective subpoints. So the metric space is the surface of the Earth and distances are spherical distances. Accordingly, we speak about the *spherical Voronoi diagram* and the *spherical Delaunay triangulation*

of  $\mathcal{O}$ . Note that that Voronoi regions are (spherical) convex polygons. Now, every point on Earth's surface belongs to a unique Voronoi region, a unique Delaunay triangle respectively (except for the case that a point is on a line of the Voronoi diagram or the Delaunay triangulation). So both  $VD(\mathcal{O})$  and  $DT(\mathcal{O})$  can be used to partition Earth's surface. For an example see Figure 4.

It should be noted that on the sphere there are no infinite Voronoi regions and that  $VD(\mathcal{O})$  can be obtained from  $DT(\mathcal{O})$  by connecting the circumcircle centers of its triangles following certain rules. And no point of  $\mathcal{O}$  is in the interior of the circumcircle of any spherical triangle of  $DT(\mathcal{O})$ .

In this paper, we compute the Delaunay triangulation basically using the approach of [34] and then generate the Voronoi diagram from it. By subdividing the target area into several adjacent convex polygons, the constellation coverage problem can be decomposed into a set of single satellite coverage problems.

## B. Orientation Angle

Consider a spherical circle  $\Theta(P, \alpha)$  with center point  $P(\theta, \varphi)$  and radius  $\alpha$ , where  $\theta$  and  $\varphi$  are the longitude and latitude of  $P$ , respectively. Let us rotate the coordinates such that in the new coordinate system, the  $x$ -axis passes through the center  $P'$  of the rotated spherical circle. The coordinate rotation matrix is

$$P' = \mathcal{M}(P) = R_y(-\varphi)R_z(\theta), \quad (3)$$

where  $\mathcal{M} \in \mathbb{R}^{3 \times 3}$  with

$$R_z(\theta) = \begin{bmatrix} \cos(\theta) & -\sin(\theta) & 0 \\ \sin(\theta) & \cos(\theta) & 0 \\ 0 & 0 & 1 \end{bmatrix} \text{ and } R_y(-\varphi) = \begin{bmatrix} \cos(\varphi) & 0 & -\sin(\varphi) \\ 0 & 1 & 0 \\ \sin(\varphi) & 0 & \cos(\varphi) \end{bmatrix}.$$

Figure 3 gives an illustration of the spherical circle  $\Theta'$  after the rotation  $\mathcal{M}(\Theta) = \{\mathcal{M}(Q) \mid Q \in \Theta\}$ , where now the  $x$ -axis passes through the center  $P' = (0, 0)$  of the rotated spherical circle.

The *orientation angle* with respect to  $P'$  of any point in the rotated spherical circle is denoted by  $\beta$ . It is clear that the orientation angle of any point  $Q' = (x, y, z)$ ,  $x \neq 0$ , in the rotated spherical circle is

$$\beta = \arctan\left(\frac{z}{y}\right). \quad (4)$$

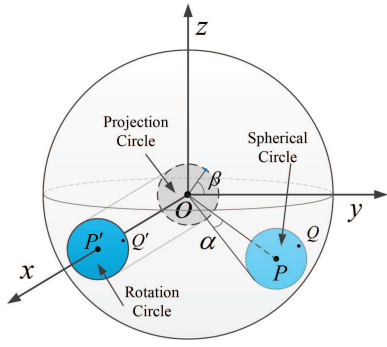


Fig. 3: Orientation angle

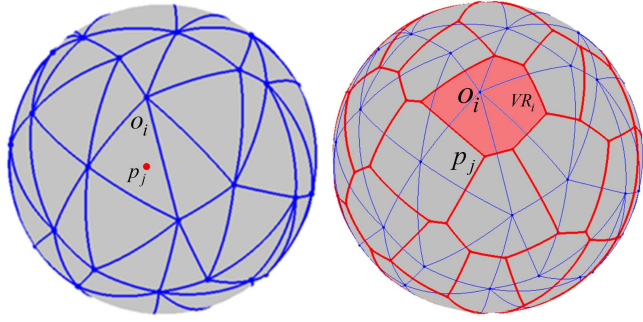


Fig. 4: Construction of coverage area for a constellation

computation using projection.

There is a *natural* mapping, which we denote  $h$ , that projects the spherical circle  $\Theta'$  onto the  $yz$ -plane. Since there exists a one-to-one mapping  $g$  that assigns to each orientation angle  $\beta \in [0, 2\pi)$  a unique point in  $h(\Theta')$ , it is clear that the projection  $h(\Theta')$  is a circle on the  $yz$ -plane. Hence,  $g$  maps an angle  $\beta \in [0, 2\pi)$  to  $g(\beta) = (0, \cos \beta, \sin \beta)$ . The inverse projection  $f$  mapping an orientation angle to a point on the original spherical circle  $\Theta$  maps  $\beta \in [0, 2\pi)$  to  $\mathcal{M}^{-1}(\cos \alpha, \sin \alpha \cos \beta, \sin \alpha \sin \beta)$ , where  $\mathcal{M}^{-1}$  denotes the inverse of the rotation mapping (3). Note that  $f$  can also be expressed as  $f = \mathcal{M}^{-1} \circ h^{-1} \circ g$ .

## V. Constellation Coverage Analysis

A key issue for the design of satellite orbits and for the evaluation of the performance of constellations is the accurate computation and analysis of the coverage for a given target area  $\Omega$ . This topic is addressed in this section where we give some definitions relating the Voronoi diagram computed for a constellation  $\mathcal{C} = \{S_1, S_2, \dots, S_N\}$  of  $N$  satellites to its coverage properties. First we focus on one satellite  $S_i$  and later extend the concepts to the full constellation. As before, we denote by  $\mathcal{O} = \{O_1, O_2, \dots, O_N\}$  the set of subpoints of the constellation.

- 1) The *coverage target area*  $\Omega_i$  of  $S_i$  is the intersection of the Voronoi region  $VR(O_i)$  and the target area  $\Omega$ . If  $\Omega$  is a polygon, then  $\Omega_i$  is also a polygon. Its vertices are all the vertices of  $VR(O_i)$  in the target area plus some "new" vertices generated by the intersection of the boundary of  $VR(O_i)$  with the spherical arcs that define  $\Omega$ .

- 2) The *maximum circle radius of  $S_i$*  is the maximum spherical distance between  $O_i$  and any point in its coverage target area  $\Omega_i$ .
- 3) A *coverage feature point* of  $S_i$  is any point on the boundary of  $\Omega_i$  that potentially could be of maximum distance to  $O_i$ . The set of feature points of  $S_i$  is denoted by  $F_i$ . Indeed  $F_i$  contains all the vertices of  $\Omega_i$ . Furthermore, when some of the lines that define  $\Omega$  are small arcs, then  $F_i$  may contain additional points, corresponding to the properties and intersection characteristics of small arcs.

From the above definitions it follows that for any point in  $\Omega_i$ ,  $1 \leq i \leq N$ , the subpoint  $O_i$  is a nearest subpoint among all subpoints of the satellites. Furthermore, all the coverage target areas only intersect in boundary points, as they are defined as subsets of Voronoi regions.

#### A. Construction of the Coverage Target Area

The coverage area of one satellite can be studied directly according to equation (1). Suppose now that the target area  $\Omega$  must be covered by a constellation  $\mathcal{C} = \{S_1, S_2, \dots, S_N\}$ . In order to obtain the coverage area of  $\mathcal{C}$  we compute the Voronoi diagram for the subpoints  $\mathcal{O} = \{O_1, O_2, \dots, O_N\}$  and the coverage target areas  $\Omega_i$  together with the feature points  $F_i$ . As an example see Figure 4 giving the Voronoi diagram and Delaunay triangulation for the Walker constellation [6] with the configuration parameters  $(T/P/F) = (48/8/1)$  and orbital inclination  $Incl = 52^\circ$ .

Full coverage of a target area  $\Omega$  is attained by a constellation if each satellite has full coverage of its coverage target area  $\Omega_i$ . When some  $S_i$  does not have full coverage of  $\Omega_i$ , then no other satellite can cover any point in the uncovered part of  $\Omega_i$ . In this case, the constellation cannot totally cover  $\Omega$ .

As a consequence of the above analysis, after the Voronoi diagram of  $\mathcal{O}$  has been obtained, the constellation full coverage problem for a target area  $\Omega$  is equivalent to a series of  $N$  independent coverage problems, each of them restricted to its own target area  $\Omega_i$ . The region  $\Omega_i = VR(O_i) \cap \Omega$ , is a spherical polygon. The boundary  $\partial\Omega_i$  is composed of several spherical great and small arc segments, which are generated according to the intersection of  $VR(O_i)$  with  $\Omega$ , and the orientation angle of the feature point. The spherical arc is denoted as *great arc segments* if the center of the

corresponding spherical circumcircle is  $O_e$ , and as *small arc segments* otherwise.

Therefore, the question that arises now is how to determine whether or not a given satellite  $S_i$  has full coverage of its target area  $\Omega_i$ . The answer is given in terms of the coverage of feature points. Let  $F_i = \{f_{i1}, f_{i2}, \dots, f_{im}\}$  be the set of feature points of  $S_i$  and  $r_{ij}$  be the spherical distance from subpoint  $O_i$  to feature point  $f_{ij}$ . The maximum circle radius of  $S_i$  is

$$r_{\max}(i) = \max\{r_{i1}, r_{i2}, \dots, r_{im}\}. \quad (5)$$

Thus, the re-statement of condition (2) for full coverage of the target area  $\Omega$  by constellation  $\mathcal{C}$  is

$$d \geq r_{\max} = \max\{r_{\max}(1), r_{\max}(2), \dots, r_{\max}(N)\}, \quad (6)$$

where, as before,  $d$  denotes the spherical radius of the coverage areas of the satellites for the coverage angle  $\alpha$  associated with a minimum elevation angle  $\gamma_{\min}$ , i.e.,  $d = R_e \alpha$ .

#### Calculation of the Coverage Feature Points

Feature points play a crucial role in the coverage problem of a constellation for a target area. Each coverage target area is given by the set of feature points on the Earth's surface with shortest distance to the subpoint of a satellite. In some cases, which we list below, it is possible to easily compute the set of feature points of a given satellite.

- 1) If the coverage target area  $\Omega_i$  of  $S_i$  is empty, then  $S_i$  has no coverage feature point and  $F_i = \emptyset$ .
- 2) If the boundary  $\partial\Omega_i$  of the coverage area of satellite  $S_i$  contains arc segments of spherical great circles, and does not contain any small arc segment, then the set of feature points  $F_i$  is given by the intersection points of adjacent arc segments of  $\partial\Omega_i$ , as depicted in Fig. 5. Suppose that great arcs  $\widehat{AB}$  and  $\widehat{CD}$  on the spherical great circle with center point  $O$  and radius  $R_e$  belong to  $\partial\Omega_i$  and that we also have the spherical small circles  $(O_1, r_1)$  and  $(O_2, r_2)$  with subpoints  $O_1$  and  $O_2$  and respective radii  $r_1$  and  $r_2$  satisfying  $r_1 < R_e$  and  $r_2 < R_e$ . Let us further assume that  $(O_1, r_1)$  covers points  $A$  and  $B$ , and  $(O_2, r_2)$  covers points  $C$  and  $D$ . Because the curvature of the spherical great circle is smaller than that of the spherical small circle, we have  $\frac{1}{R_e} < \frac{1}{r_1}$  and  $\frac{1}{R_e} < \frac{1}{r_2}$ . Thus, arcs  $\widehat{AB}$  and  $\widehat{CD}$  must be inside the circles  $(O_1, r_1)$  and

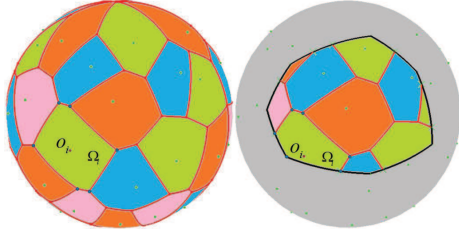
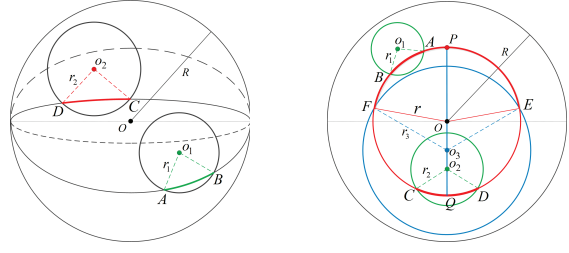


Fig. 5: Subdivision of target area only with great arcs (like global target area and spherical polygon area).



(a) Great arcs intersection. (b) Small arcs intersection.

Fig. 6: Spherical arcs intersections.

$(O_2, r_2)$ , respectively. It is obvious that the point of maximum distance to center point  $O_1$ , among all the points on arc  $\widehat{AB}$ , is either  $A$  or  $B$ . The same holds with  $C$  and  $D$  for arc  $\widehat{CD}$  relative to  $O_2$  (see Figure 6a).

- 3) If the boundary  $\partial\Omega_i$  of the coverage area belonging to satellite  $S_i$  contains a small arc segment  $\widehat{\Theta}$ , then, in addition to the points defined in the above item, we add to  $F_i$  the intersection points of the adjacent small arc segments, as depicted in Figure 7.

Suppose now that small arcs  $\widehat{AB}$ ,  $\widehat{CD}$ , and  $\widehat{EF}$  on a spherical small circle  $(O, r)$  belong to  $\partial\Omega_i$ . Let us also assume that there is another spherical small circle  $(O', r')$ , where  $O'$  is the subpoint and  $r' < R_e$  (see Figure 6b). When the distance between  $O'$  and  $O$  is greater than or equal to  $r$ , then all of the points on the small arc  $\widehat{AB}$  are inside  $(O', r')$ , provided that the spherical small circle  $(O', r')$  covers both  $A$  and  $B$  (see  $(O_1, r_1)$  in Figure 6b). Otherwise, two different cases may arise. In the first case we have that  $\frac{1}{r} \leq \frac{1}{r'}$  (see spherical small circle  $(O_2, r_2)$  in Figure 6b). Then, full coverage of the small arc  $\widehat{CD}$  is implied by coverage of both  $C$  and  $D$ . In the second case  $\frac{1}{r} > \frac{1}{r'}$  (see spherical small circle  $(O_3, r_3)$  in Figure 6b). Then, neither  $E$  nor  $F$  are of longest distance to  $O'$  among the points on  $\widehat{EF}$ . Now, to obtain such a maximum distance point, we connect  $O_3$  with  $O$  and extend this arc to a spherical great circle, which intersects with the spherical small circle  $(O, r)$  in points  $P$  and  $Q$ . Indeed it can be shown that the point of maximum distance to  $O_3$  is either  $P$  or  $Q$ , provided that they are on

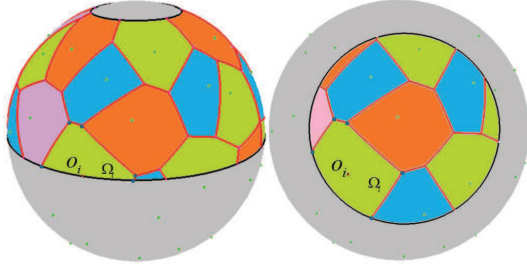


Fig. 7: Subdivision of target area with small arcs (like latitude target area and spherical circle target area).

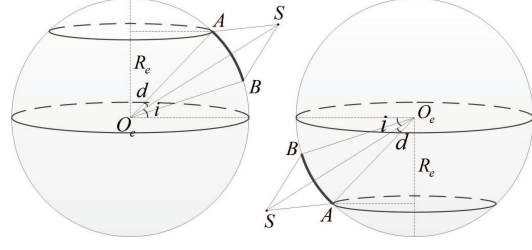


Fig. 8: Satellite coverage in the ECI reference frame.

arc  $\widehat{EF}$ . Such a maximum distance point also becomes one of the feature points of subpoint  $O_3$ .

## B. Continuous Coverage Analysis of Constellations

The analysis of full coverage of a target area  $\Omega$  by a constellation  $\mathcal{C}$  at a fixed time point performed above can be easily extended to study the continuous coverage of  $\Omega$  by  $\mathcal{C}$  over a given reconstruction period. Indeed, the necessary and sufficient condition that guarantees that  $\mathcal{C}$  offers continuous full coverage for  $\Omega$  throughout the given reconstruction period is that (6) holds at any time of the reconstruction period. Hence, for this analysis we will discretize the reconstruction period and check the condition at each time point of the discretized reconstruction period.

Observe, that the position of each satellite changes as time varies, as it *moves* through different points of its orbit. Hence the subpoint of each satellite also depends on the time  $t$ , and accordingly on the set of subpoints  $O^t = \{O_1^t, O_2^t, \dots, O_N^t\}$ . That is, for a given minimum elevation angle  $\gamma_{\min}$ , the coverage angle  $\alpha^t$  obtained with expression equation (1) together with the associated spherical radius  $d^t = R_e \alpha^t$ , depend on  $t$ . This means that, in order to check whether or not condition (6) holds at any time of the reconstruction period, the construction must be repeated for each time point of the reconstruction period, including the procedure for obtaining the Voronoi diagram, the target areas of the different satellites, and their feature points. Hence, the condition that guarantees full coverage for  $\Omega$  throughout the reconstruction period is  $d^t = R_e \alpha^t \geq r_{\max}^t$ , for all  $t$  in the discretized reconstruction period.

## VI. Satellite Orbital Parameters Calculation

In the previous sections we have seen that the spherical geometric subdivision based on Voronoi diagrams allows to address the continuous full coverage problem, i.e., the problem of determining whether or not a given configuration for a satellite constellation provides continuous full coverage for a given target area.

As we see below, the proposed geometric subdivision can also be used to address the problem of finding a constellation of  $N$  satellites that provides full coverage for a given target area. As it is known, there are several orbital parameters that define the properties of a constellation of satellites. Eccentricity and perigee are typically fixed in the design of circular orbital parameters, so they need not be computed. Moreover, the initial values of the RAAN and Mean Anomaly are not considered to be important in the continuous coverage problem, so they can be distributed evenly. On the other hand, it is well-known that Walker's configuration [6] produces constellations with good symmetry and stability properties. Hence for the design of a constellation for the continuous coverage problem, we will follow Walker's configuration and assume that satellites are distributed in a uniform way. As a result, only the length of the semi-major axis (altitude  $h$ ) and the inclination angle  $Incl$  offer some freedom of choice for orbital design. Below, we show how to obtain these parameters. For our analysis we recall that, for any two satellites in the constellation, the relative motion trajectory in space changes periodically. Therefore, the values of orbital inclination and maximum coverage circle radius, satisfying continuous coverage to target, change continuously in the constellation reconstruction period.

### A. Calculation of Orbital Altitude

As we have seen, in order to obtain continuous full coverage for the target area in the reconstruction period, condition (6) must hold at any time. That is, for a given minimum elevation angle  $\gamma_{\min}$ , at each time instant  $t$  of the reconstruction period, the spherical radius  $d^t = R_e \alpha^t$  associated with the coverage angle  $\alpha^t$  obtained with equation (1) must be such that condition (6) holds.

Next we explain how to analytically compute a value for the altitude of the satellites in the constellation that guarantees the above condition. For each time point  $t$  we obtain the set of subpoints  $\mathcal{O}^t$  and the Voronoi diagram of the satellites constellation. Then, for each satellite  $S_i \in S$ ,



we compute its set of feature points  $F_i^t$ , the spherical distances  $r_{ij}^t$  from the subpoints to their feature points, and its circle radius value  $r_{\max}^t(i)$ . Finally we compute the maximum circle radius for the constellation  $r_{\max}^t = \max\{r_{\max}^t(i) \mid 1 \leq i \leq N\}$ .

Since condition (6) holds when  $d^t = R_e \alpha^t \geq r_{\max}^t$  for all  $t$ , we compute the maximum radius  $r_{\max} = \max\{r_{\max}^t \mid t \in T\}$ . Then, we take as spherical radius  $d = \max\{d^t \mid t \in T\}$ , associated with the coverage angle  $d = \max\{\alpha^t \mid t \in T\} = r_{\max}/R_e$ .

From equation (1) we obtain

$$h = \frac{R_e \cos(\gamma_{\min})}{\cos(\frac{r_{\max}}{R_e} + \gamma_{\min})} - R_e \quad (7)$$

as altitude for the satellites in the constellation.

## B. Calculation of Orbital Inclination

It is well-known that the optimal orbital inclination corresponds to the minimum value of the maximum coverage circle radius in the constellation reconstruction period.

Suppose that the coverage target area is located in the latitude region  $[\phi_l, \phi_u]$ . The maximum latitude value of a point in the target area is  $\phi_{\max} = \max\{|\phi_l|, |\phi_u|\}$ . Therefore, for the full coverage of the target area, the satellite must cover the point with maximum latitude  $\phi_{\max}$ . Using (1), the minimum orbital inclination, for a given orbital altitude  $h^t$  and minimum observation elevation angle  $\gamma_{\min}$ , is given by

$$Incl_{\min}^t = \max\{\phi_{\max} - \alpha^t, 0\}. \quad (8)$$

Figure 8 illustrates the satellite coverage of the Earth's surface in the Earth-centered inertial (ECI) reference frame. It reflects the coverage status when the satellite passes through the highest and lowest points in the ECI frame.

## VII. Computational Experiments

In this section we analyze the Globalstar mobile satellite system, designed by Loral and Qualcomm of America, with the geometric subdivision method proposed in this paper. This system is a Walker constellation with configuration parameters  $(T/P/F) = (48/8/1)$ . Note that in this notation  $T$  denotes the total number of satellites and not the reconstruction time period. The satellite orbital

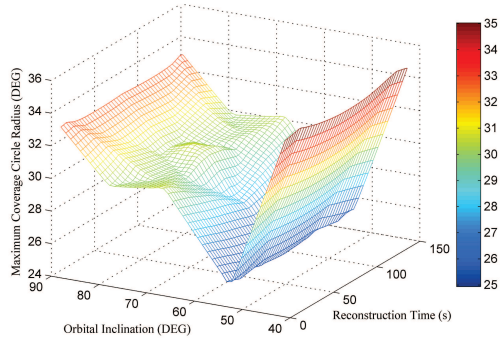
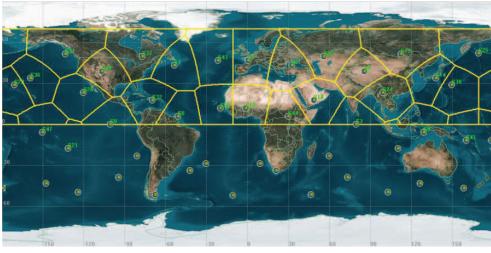


Fig. 9: Spherical subdivision for the Globalstar system. Fig. 10: Maximum coverage circle radius with orbital inclination angle over time.

inclination is  $Incl = 52^\circ$  and the altitude is  $h = 1414$  km. It provides single continuous full coverage of the latitude region  $[S70^\circ, N70^\circ]$  with a minimum coverage elevation angle  $\gamma_{\min} = 10^\circ$  [5]. In our study we use a discretized reconstruction period of 142.6 s.

### A. Subdivision

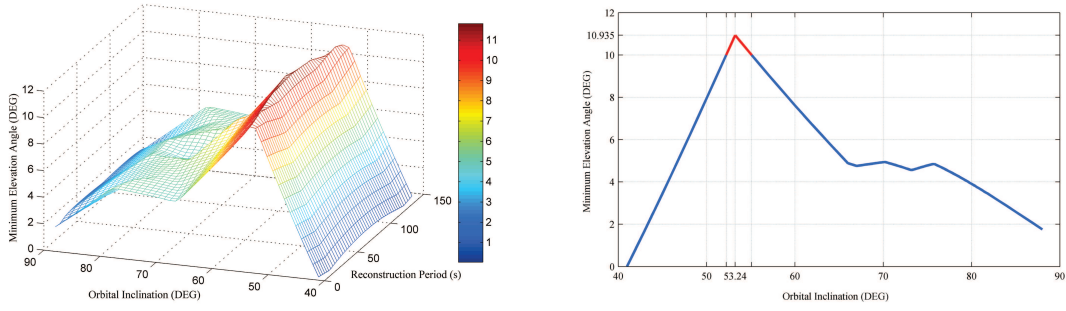
Because of the symmetry property of Walker constellations we only need to analyze the coverage capacity of the Globalstar system for the latitude region  $[0^\circ, N70^\circ]$ . The construction of the Voronoi diagram at  $t = 2015-01-01$  00:00:00 is shown in Figure 9, where every convex polygon in the graph corresponds to the coverage area of a satellite.

### B. Coverage Calculation

#### 1. Analysis of System Configuration Parameters

We re-optimize the orbital inclination according to (8) under the assumption that all other parameters are given and fixed. Then, we use (6) to calculate the value of the coverage circle radius, satisfying the continuous full coverage of the latitude region. The results are given in Figure 10. It illustrates the variation of the maximum coverage circle radius relative to the orbital inclination angle at different times of the reconstruction period when full coverage is imposed.

The results of the computations of the minimum elevation angle corresponding to the maximum coverage circle radius that satisfies the coverage demand are depicted in Figure 11. Figure 11a illustrates the variation of the minimum elevation angle with respect to the orbital inclination



(a) Minimum elevation angle with respect to orbital inclination over time (full coverage). (b) Minimum elevation angle with respect to orbital inclination (full coverage).

Fig. 11: Variation of the minimum elevation angle relative to orbital inclination.

angle, at different times under the full coverage constraint. Figure 11b shows the variation of the minimum elevation angle with respect to the orbital inclination under the constraint of continuous full coverage. From the above results we can conclude the following.

- 1) In order to satisfy the continuous full coverage of the latitude region under the constraint of minimum elevation angle  $\gamma_{\min} = 10^\circ$ , the satellite orbital inclination is in the range  $[52.224^\circ, 55.094^\circ]$ . So with the original system configuration parameter  $Incl = 52^\circ$  the latitude region  $[S70^\circ, N70^\circ]$  cannot be covered completely.
- 2) Figures 10 and 11 give optimal inclination values. It can be seen that the maximum coverage circle radius is  $r_{\max} = 25.586^\circ$  and the minimum elevation angle is  $\gamma = 10.935^\circ$ , while the orbital inclination is  $Incl = 53.24^\circ$ .

Therefore, the configuration  $(T/P/F) = (48/8/1)$  with inclination  $Incl = 53.24^\circ$  can be regarded as the best constellation configuration parameters given the continuous full coverage requirements for the latitude region. In this context the minimum orbital altitude value is  $h = 1347.679$  km.

Suppose now that all the constellation parameters are constant. Figure 12 gives the maximum coverage gap of the constellation for different latitude regions. The  $x$ -axis represents time in the constellation reconstruction period and the  $y$ -axis gives the upper bound values of the latitude regions  $[0^\circ, y^\circ]$  in the graph. The shaded area indicates coverage gap intervals in different latitude regions. For example, the coverage gap interval during the reconstruction period for the latitude

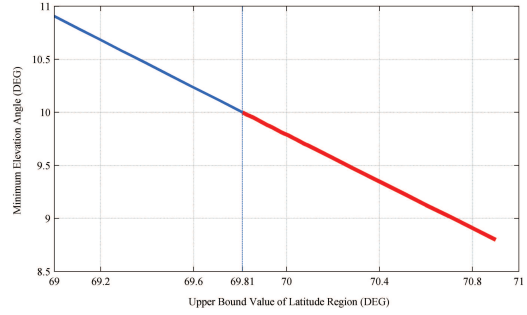
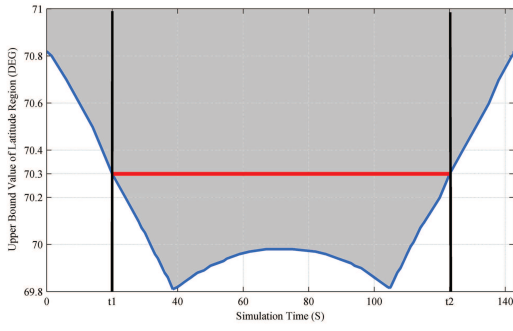


Fig. 12: Maximum coverage gap of constellation in different latitude regions.

Fig. 13: Minimum elevation angle with different latitude regions imposing continuous full coverage.

region  $[0^\circ, N70.3^\circ]$  is  $[t_1, t_2]$ .

Further results are presented in Figure 13 on the former basis giving the variation of the minimum elevation angle for different latitude regions under the constraint of continuous full coverage. The  $x$ -axis represents the upper bound value  $[0^\circ, x^\circ]$  of the latitude regions. The  $y$ -axis represents the minimum elevation angle under the constraint of continuous full coverage. It is clear that the original constellation configuration parameters can only offer single continuous full coverage for the latitude region  $[S69.81^\circ, N69.81^\circ]$  or less.

## 2. Efficiency Analysis

For the same target area  $[0^\circ, N70^\circ]$  of the latitude region we compared the computational efficiency of our new coverage method with the classical grid-point technique and the longitude strip method. For the analyzed data, the computing time needed by our method is only 20 ms and does not change with the constellation and the type and size of coverage area. The computational results for the grid-point technique and the longitude strip method are depicted in Figure 14. The  $x$ -axis indicates the partition precision, given as the number of longitude strips or grid-points in 1 km on Earth's surface. The  $y$ -axis shows the instantaneous coverage computing time for the latitude region with the Globalstar system. Given that the grid-point technique and the longitude strip method are both numerical simulation methods, their major drawback is that results with

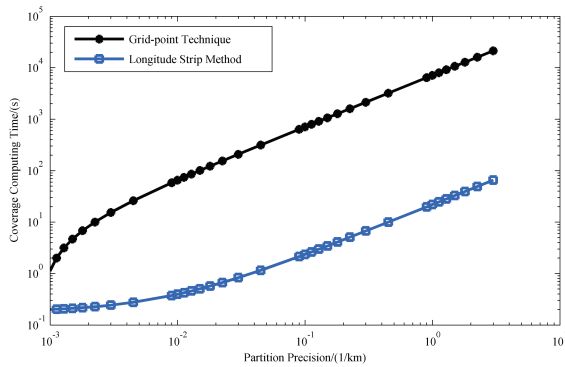


Fig. 14: Coverage computation times in relation to the partition precision.

high accuracy can only be obtained with a considerable increase in computing times and memory requirements.

The computations show that the optimal system parameters obtained with our method are basically the same as the original parameters produced by the Globalstar system.

### VIII. Conclusions

In this paper we have proposed a new method based on spherical geometric subdivision for the analysis of the continuous coverage of satellites and the calculation of satellite orbital parameters for the full coverage problem. The proposed method is exact for fixed time  $t$  and works on any type of coverage target areas. Though only approximate in the constellation reconstruction period, it is also very effective for evaluating a series of further meaningful performance indices for the continuous and the discontinuous coverage problem. (Note the exception, that when computing the spherical Delaunay subdivision not all subpoints must be located in the same semi-spherical surface since, otherwise, the subdivision is invalid.)

The new proposed method also produces analytical solutions as well as the range for each parameter value so as to satisfy the coverage requirements. The satellite orbital parameters can be obtained directly from the maximum coverage circle radii. Moreover, optimal satellite orbital inclinations and altitudes can be obtained according to the original design objectives. Experimental results also indicate that traditional methods based on grid-point division or longitude strip partition are usually unsuitable for very large regions under high accuracy requirements.

Summarizing, the decision space for an optimal constellation design is reduced considerably, and the constellation design process improves significantly.

### Acknowledgments

This work was supported by National Natural Science Foundation of China under Grant No. 41571403 and No. 61472375.

### References

- [1] Rainer, S., Klaus, B., and Marco, D. E. "Small Satellites for Global Coverage: Potential and Limits," *ISPRS Journal of Photogrammetry and Remote Sensing*, Vol. 65, No. 6, Sep. 2010, pp. 492–504.
- [2] Sandau, R., "Status and Trends of Small Satellite Missions for Earth Observation," *Acta Astronautica*, Vol. 71, No. 1, Jan. 2010, pp. 1–12.
- [3] Zhao, Z.Y., Cai, Y. W., Zhao, Y. B., and Li, Y. "Research on Small Satellite Formation Scheme for Earth Observation Task," *Proceedings of the 2015 International Conference on Automation, Mechanical Control and Computational Engineering*, Atlantis Press, Paris, France, April 2015, pp. 1678–1683.
- [4] Y. Ulybyshev, "Satellite Constellation Design for Complex Coverage," *AIAA Journal of Spacecraft and Rockets*, Vol. 45, No. 4, Jul. 2008, pp. 843–849.
- [5] Crowe, K. E. and Raines, R. A. "A Model to Describe the Distribution of Transmission Path Elevation Angles to the Iridium and Globalstar Satellite Systems," *IEEE Communications Letters*, Vol. 3, No. 8, Aug. 1999, pp. 242–244.
- [6] Walker, J. G. "Circular Orbit Patterns Providing Continuous Whole Earth Coverage," *Royal Aircraft Establishment*, U.K., Technique Report 70211, Nov. 1970.
- [7] Crossley, W. A. and Williams, E. A. "Simulated Annealing and Genetic Algorithm Approaches for Discontinuous Coverage Satellite Constellation Design," *Engineering Optimization*, Vol. 32, No. 3, 2000, pp. 353–371.
- [8] Asvial, M., Tafazolli, R., and Evans, B. G. "Satellite Constellation Design and Radio Resource Management using Genetic Algorithm," *IEE Proceedings-Communications*, Vol. 151, No. 3, 6 Jul. 2004, pp. 204–209.
- [9] Ferringer, M. P., and Spencer, D. B. "Satellite Constellation Design Tradeoffs using Multiple-Objective Evolutionary Computation," *AIAA Journal of Spacecraft and Rockets*, Vol. 43, No. 6, Nov. 2006, pp. 1404–1411.

- [10] Wang, L., Wang, Y., Chen, K., and Zhang, H. "Optimization of Regional Coverage Reconnaissance Satellite Constellation by NSGA-II Algorithm," *Proceedings of the 2008 IEEE International Conference on Information and Automation*, IEEE, Piscataway, New Jersey, USA, Jun. 2008, pp. 1111–1116.
- [11] Ferringer, M. P., Clifton, R. S., and Thompson, T. G. "Efficient and Accurate Evolutionary Multi-Objective Optimization Paradigms for Satellite Constellation Design," *AIAA Journal of Spacecraft and Rockets*, Vol. 44, No. 3, May. 2007, pp. 682–691.
- [12] Jiang, Y., Zhang, G., Li, G., Xie, Z., and Yang, S. "Study on Orthogonal IGSO Global Communication Satellite Constellation," *IEEE 6th International ICST Conference on Communications and Networking in China (CHINACOM)*, Aug. 2011, pp. 1064–1068.
- [13] Ma, D. M., Hong, Z. C., Lee, T. H., and Chang, B. J. "Design of a Micro-Satellite Constellation for Communication," *Acta Astronautica*, Vol. 82, No. 1, Jan. 2013, pp. 54–59.
- [14] Lluch, I., and Golkar, A. "Satellite-to-Satellite Coverage Optimization Approach for Opportunistic Inter-Satellite Links," *IEEE Aerospace Conference*, IEEE, Piscataway New Jersey, USA, Mar. 2014, pp. 1–13.
- [15] Morrison, J. J. "A System of Sixteen Synchronous Satellites for Worldwide Navigation and Surveillance," *Technical Department of Transportation Federal Aviation Administration Systems Research and Development Service, Washington D. C.*, Mar. 1973.
- [16] Jiang, Y., Yang, S., Zhang, G., and Li, G. "Coverage Performances Analysis on Combined-GEO-IGSO Satellite Constellation," *Journal of Electronics (China)*, Vol. 28, No. 2, Mar. 2011, pp. 228–234.
- [17] Mortari, D., Sanctis, M. D., and Lucente, M. "Design of Flower Constellations for Telecommunication Services," *Proceedings of the IEEE*, Vol. 99, No. 11, Jul. 2011, pp. 2008–2019.
- [18] Casten, R. G., and Gross, R. P. "Satellite Cumulative Earth Coverage," *AIAA Astrodynamics Specialist Conference*, Univelt, San Diego, California, USA, Vol. 1, Aug. 1981.
- [19] Xu, M., and Huang, L. "An Analytic Algorithm for Global Coverage of the Revisiting Orbit and its Application to the CFOSAT Satellite," *Astrophysics and Space Science*, Vol. 352, No. 2, Aug. 2014, pp. 497–502.
- [20] Ulybyshev, Y. "Geometric Analysis of Low-Earth-Orbit Satellite Communication Systems: Covering Functions," *AIAA Journal of Spacecraft and Rockets*, Vol. 37, No. 3, May. 2000, pp. 385–391.
- [21] Seyedi, Y. and Safavi, S. M. "On the Analysis of Random Coverage Time in Mobile LEO Satellite Communications," *IEEE Communications Letters*, Vol. 16, No. 5, 23 Mar. 2012, pp. 612–615.
- [22] Ballard, A. H. "Rosette constellation of earth satellite," *IEEE Transaction on Aerospace and Electronic Systems*, Vol 16, No. 5, Sep. 1980, pp. 656–673.

- [23] Sarno, S., Graziano, M.D., and D'Errico, M., "Polar Constellations Design for Discontinuous Coverage," *Acta Astronautica*, Vol. 127, Oct. 2016, pp. 367–374.
- [24] Li, T., Xiang, J., Wang, Z., and Zhang, Y., "Circular Revisit Orbits Design for Responsive Mission over a Single Target", *Acta Astronaut*, Vol. 127, Oct. 2016, pp. 219–225.
- [25] Mozhaev, G. V. "Capabilities of Kinematically Regular Satellite Systems with Symmetry Groups of the Second Type in the Problem of Continuous Single Coverage of the Earth," *Cosmic Research*, Vol. 43, No. 3, May. 2005, pp. 205–212.
- [26] Ulybyshev, Y. "Geometric Analysis and Design Method for Discontinuous Coverage Satellite Constellations," *AIAA Journal of Guidance, Control, and Dynamics*, Vol. 37, No. 4, 5 Feb. 2014, pp. 549–557.
- [27] Ulybyshev, Y.P., "A General Analysis Method for Discontinuous Coverage Satellite Constellations," *AIAA Journal of Guidance, Control, and Dynamics*, Vol. 38, No. 12, Aug. 2015, pp. 2475–2482.
- [28] Razoumny, Y.N., "Fundamentals of the Route Theory for Satellite Constellation Design for Earth Discontinuous Coverage. Part1: Analytic Emulation of the Earth Coverage," *Acta Astronautica*, Vol. 128, July. 2016, pp. 722–740.
- [29] Mohammadi, L. "Determination of the Best Coverage Area for Receiver Stations of LEO Remote Sensing Satellites," *Proceedings of the 2008 3rd International Conference on Information and Communication Technologies: From Theory to Applications*, IEEE, Piscataway, New Jersey, April 2008, pp. 1–4.
- [30] Sengupta, P., Vadali, R. S., and Alfriend, T. K. "Satellite Orbit Design and Maintenance for Terrestrial Coverage," *AIAA Journal of Spacecraft and Rockets*, Vol. 47, No. 1, Jan. 2010, pp. 177–187.
- [31] Devillers, O. "Delaunay Triangulation and Randomized Constructions," *Springer Encyclopedia of Algorithms*, Springer US, Oct. 2014, pp. 1–7.
- [32] Okabe, A., Boots, B., Sugihara. K., and Chui, S. N. "Spatial Tessellations: Concepts and Applications of Voronoi Diagrams," *John Wiley and Sons*, Vol. 501, 2009, pp. 46–105.
- [33] Zhao, M., An, B., Wu, Y., Chen, B., and Sun, S. "A Robust Delaunay Triangulation Matching for Multispectral/Multidate Remote Sensing Image Registration," *IEEE Geoscience and Remote Sensing Letters*, Vol. 12, No. 4, Apr. 2015, pp. 711–715.
- [34] Zhou, L., Huang, D., Li, C., and Zhou, D., "Algorithm for GPS Network Construction Based on Spherical Delaunay Triangulated Irregular Network," *Journal of Southwest Jiaotong University*, Vol. 42, No. 3, Jun. 2007, pp. 380-383.
- [35] Jacobsen, D. W., Gunzburger, M., Ringler, T., Burkardt, J., and Peterson, J. "Parallel Algorithms for Planar and Spherical Delaunay Construction with an Application to Centroidal Voronoi Tessellations,"



*Geoscientific Model Development*, Vol. 6, No. 4, 6 Dev. 2013, pp. 1353–1365.

- [36] Yan, D. M., Wang, W., Levy, B. and Liu, Y. "Efficient Computation of Clipped Voronoi Diagram for Mesh Generation," *Computer-Aided Design*, Vol. 45, No. 4, Apr. 2013, pp. 843–852.
- [37] Peterka, T., Morozov, D. and Phillips, C. "High-Performance Computation of Distributed-Memory Parallel 3D Voronoi and Delaunay Tessellation," *Proceedings of the International Conference for High Performance Computing, Networking, Storage and Analysis*, IEEE, Piscataway, New Jersey, USA, Nov. 2014, pp. 997–1007.